Polarization of photon echoes from SF_6 molecules

C. V. Heer and R. J. Nordstrom
Department of Physics, Ohio State University, Columbus, Ohio 43210
(Received 10 June 1974; revised manuscript received 14 August 1974)

We measured the polarization of the photon echo which was stimulated in a gas of SF_6 molecules by either linear-linear, circular-linear, or linear-circular pulse sequences from the $P(14)$, $P(16)$, $P(18)$, $P(20)$, $P(22)$, and $P(24)$ CO_2 laser lines near 10.4 μm. For $P(16)$ a linear-linear pulse sequence with angle β between the linearly polarized pulses produced a linearly polarized echo at angle φ with the second pulse, and φ rotated in the same sense as β; a left-circular–linear sequence produced an echo with right elliptic polarization, and a linear–left-circular sequence produced an echo with left-circular polarization. For all other lines a linear-linear sequence produced an echo polarized along the second pulse, and results were similar to the measurement of Gordon *et al.* on $P(20)$. For $P(14)$, $P(18)$, and $P(20)$ a circular-linear sequence produced an echo linearly polarized along the second pulse. For $P(14)$ through $P(20)$ a linear–left-circular sequence produced a left-circular echo. A theory is developed for these pulse sequences for arbitrary values of angular momentum J_a, and a simplification found for large J_a. For laser radiation in direction Y and the linear polarization of the second pulse along Z, the polarization vector for a linear-linear sequence is approximately $\mp(1/2)\,\hat{X}\sin\beta + \hat{Z}\cos\beta$, and for a left-circular–linear sequence $\pm(i/2)\,\hat{X} + \hat{Z}$, where the upper sign refers to $J_a = J_b \pm 1$ or the P and R branches and the lower sign to $J_a = J_b$ or Q branch. For a linear–left-circular sequence the echo is left circular for $J_a = J_b$, $J_b \pm 1$ or the P, Q, and R branches. The general features of the linear-linear sequence are similar to those suggested by Gordon *et al.* when a sign ambiguity is considered. Only $P(16)$ was in good agreement with theory. The $-(1/2)\,\hat{X}\sin\beta$ or the $+(i/2)\hat{X}$ terms were not observed for the other lines.

I. INTRODUCTION

A reasonably detailed theory of photon echoes is given and the terms which give rise to the anomalous polarization of the photon echo, the wavefront curvature of the photon echo, etc. are shown explicitly. The emphasis of this paper is on the polarization of the photon echo which is stimulated by a linearly polarized first pulse and a linearly polarized second pulse, or by circular-linear pulse sequences for molecules with large values of total angular momentum J_a. Earlier theories on photon echoes from ruby[1] or from SF_6 were confined to small values[2,3] of total angular momentum J_a for $J_a = J_b$ or $J_a = J_b \pm 1$. The paper of Gordon, Wang, Patel, Slusher, and Tomlinson[2] considered linearly polarized pulses of short duration and suggested that the intensity and linear polarization of the echo for large values of J_a would be similar to those for $J_a = 5$. For these short pulses they were able to obtain an exact solution for $J_a = J_b$ and to confirm their suggestion that large J_a behaved in a manner similar to $J_a = J_b = 5$. This paper examines the echo polarization for large values of J_a in greater detail for $J_a = J_b \pm 1$ and in somewhat greater detail for $J_a = J_b$ for linear-linear pulse sequences. A sign ambiguity which occurs between the text and Figs. 8 and 9 in the paper of Gordon *et al.* is corrected. The assumption of resonance during the exciting pulses, i.e., pulses of short duration, is not made. Since the strength of the exciting pulse depends on the axial quantum number m, both the m value and the velocity of the molecule are important in determining the echo amplitude. Detailed expressions for the electric dipole moment or echo polarization are given by Eq. (22) for a linear-linear pulse sequence, by Eq. (A1) for a circular-linear pulse sequence, and by Eq. (A3) for a linear-circular pulse sequence. These expressions can be used for any values of J_a and J_b. An important simplification occurs for large J_a, and the echo polarization is given by very simple expressions. Thus Eq. (25) provides a simple approximation for linear-linear pulse sequences, Eq. (A2) for circular-linear, and Eq. (A4) for linear-circular. The notation is kept sufficiently general so that the theory can be applied to spherical-top molecules with cubic symmetry such as SF_6 and SiF_4 and which have a Coriolis interaction between the three-fold-degenerate vibrational state and the total angular momentum.

The initial polarization studies[2] of Gordon *et al.* on SF_6 molecules used the $P(20)$ line of CO_2 lasers with linearly polarized output pulses for stimulation of the photon echo, and the $\cos^2\beta$ dependence of the linearly polarized echo intensity suggested a $J_a = 0 \rightarrow J_b = 1$ transition. Subsequent experiments by Shimizu[4] suggested that values of $J_a > 50$ were of primary importance. Photon echoes were subsequently found by Meckley and Heer[5] for the stimulation of SF_6 molecules with the $P(14)$, $P(16)$,

$P(18)$, $P(22)$, and $P(24)$ laser lines of CO_2 near 10.4 μm. This paper reports on the experimentally observed echo polarization from SF_6 molecules which were stimulated by linear-linear, circular-linear, and linear-circular pulse sequences at the $P(14)$ through $P(24)$ CO_2 laser frequencies. These measurements are compared with the appropriate earlier theory and with the theory developed in this paper.

II. THEORY FOR PHOTON ECHOES

The response of an atom or a molecule to a saturating pulse of radiation is described by the time dependent Schrödinger equation

$$i\hbar \frac{\partial \psi}{\partial t} = [H_0 + V(t)]\,\psi\,, \tag{1}$$

where the time-dependent perturbation $V(t)$ connects the states $|J_a m_a)$ and $|J_b m_b)$ of H_0. In the electric-dipole approximation the interaction of the αth atom or molecule with the radiation field is the operator $V(t) = -\vec{P}\cdot\vec{E}(\vec{r}_\alpha, t)$. For a given angular frequency ω, the amplitude, phase, polarization, and frequency are shown explicitly by writing this interaction operator as

$$V(t) = -\vec{P}\cdot[\hat{u}_\alpha E(\vec{r}_\alpha) e^{i\varphi(\vec{r}_\alpha)} e^{-i\omega t} + \text{c.c.}]\,. \tag{2}$$

If only resonant terms are kept, the operator $V(t)$ can be written

$$V(t) = -\sum_{m_a m_b} |J_a m_a)(J_b m_b|\,(m_a|\vec{P}\cdot\hat{u}_\alpha|m_b) \times \hbar E(\vec{r}_\alpha) e^{i\varphi(\vec{r}_\alpha)} e^{-i\omega t} + \text{H.c.}\,, \tag{3}$$

and this approximation is usually referred to as the rotating-wave approximation. The notation H.c. is used for Hermitian conjugate. This operator $V(t)$ can be made phase and time independent by transforming to the interaction representation,[6]

$$V_I = A^\dagger(t) V(t) A(t) = -\hbar E(\vec{r}_\alpha) \sum_{m_a m_b} |m_a)(m_b|\,(m_a|\vec{P}\cdot\hat{u}_\alpha|m_b) + \text{H.c.}, \tag{4}$$

where

$$A(t) = \exp i[\tfrac{1}{2}\varphi_0 - \tfrac{1}{2}\Delta_0 t]\,, \tag{5}$$

and the operators are given by

$$H_0 = \sum_{m_a} |m_a)(m_a|\,E(m_a) + \sum_{m_b} |m_b)(m_b|\,E(m_b)\,, \tag{6a}$$

$$\Delta_0 = \omega\left(\sum_{m_a} |m_a)(m_a| - \sum_{m_b} |m_b)(m_b|\right), \tag{6b}$$

$$\varphi_0 = \varphi(r_\alpha)\left(\sum_{m_a} |m_a)(m_a| - \sum_{m_b} |m_b)(m_b|\right). \tag{6c}$$

The indices J_a and J_b are implied, and for convenience the notation $|m_a) = |J_a m_a)$ is used. The unitary operator which describes the evolution of the system is

$$U(t, t_0) = A(t) e^{-i\xi(t-t_0)} A^\dagger(t_0)\,, \tag{7}$$

where the operator ξ is given by

$$\xi = (H_0/\hbar - \tfrac{1}{2}\Delta_0 + \tfrac{1}{2}\dot{\varphi}_0 + V_I/\hbar)\,. \tag{8}$$

$\dot{\varphi}_0 = 0$ is selected throughout this paper, and the Doppler shift for an almost plane wave is included in the definition of ω in the rest frame of the molecule.

ξ is time independent and can be diagonalized in the representation $|\mu)$, where

$$|\mu) = \sum_{m_a} |m_a)(m_a|\,\mu) + \sum_{m_b} |m_b)(m_b|\,\mu)\,. \tag{9}$$

The eigenvalues ξ_μ and the coefficients $(m|\mu)$ follow from the solution of the homogeneous set of $(2J_a+1)+(2J_b+1)$ equations,

$$\left(\frac{E(m_a)}{\hbar} - \frac{\omega}{2} - \xi_\mu\right)(m_a|\,\mu) - \hbar^{-1}\sum_{m_b} E(\vec{r}_\alpha)(m_a|\vec{P}\cdot\hat{u}_\alpha|m_b)(m_b|\,\mu) = 0\,, \tag{10a}$$

$$\left(\frac{E(m_b)}{\hbar} + \frac{\omega}{2} - \xi_\mu\right)(m_b|\,\mu) - \hbar^{-1}\sum_{m_a} E(\vec{r}_\alpha)(m_a|\vec{P}\cdot\hat{u}_\alpha|m_b)^*(m_a|\,\mu) = 0\,. \tag{10b}$$

The matrix element of the exponential operator is evaluated in this diagonal representation,

$$(m_a|e^{-i\xi\tau}|m_b) = \sum_\mu (m_a|\,\mu)(\mu|m_b) e^{-i\xi_\mu\tau}\,. \tag{11}$$

The form of H_0 implies that the axis of quantization should be selected along the direction of the time-independent electric or magnetic fields so that the energy levels $E(m)$ depend on the quantum numbers m_a and m_b. If these fields are weak and the radiation field is strong, $E(0) \ll E(\omega)$, then the axis of quantization can be selected in a manner which simplifies the solution of Eq. (10). Thus considerable simplification occurs for the special cases of linear and circular polarization.

A. Pseudo-two-level problems

The general problem simplifies in a few special cases, and these cases occur whenever the ex-

ponential operator can be written as a product of exponential operators,

$$e^{-i\xi\tau} = \prod_{m_b} e^{-i\xi(m_b)\tau}, \tag{12}$$

where the operator $\xi(m_b)$ connects only the pair of states $|m_a\rangle$ and $|m_b\rangle$. The general interaction-matrix element can be written by the use of the Wigner-Eckart theorem as

$$\langle m_a|\vec{P}\cdot\hat{u}_\alpha|m_b\rangle\hbar^{-1}E(\vec{r}_\alpha) = v_\alpha\sum_M (J_b 1 m_b M|J_a m_a)(\hat{e}_M^*\cdot\hat{u}), \tag{13}$$

where the strength of the interaction v_α is

$$v_\alpha = \hbar^{-1}E(\vec{r}_\alpha)(J_a\|P\|J_b)(2J_a+1)^{-1/2}.$$

For linear polarization $\hat{u}=\hat{e}_0$, and the axis of quantization can be selected along $\hat{u}=\hat{z}$; since only $M=0$ or $m_a=m_b$ occurs, the set of equations which are given by Eq. (10) can be treated in pairs. For either right-circular polarization, $M=-1$, or for left-circular polarization, $M=+1$, Eq. (10) reduces to pairs when the axis of quantization $\hat{Z}$ is chosen along the direction of the laser radiation $\hat{k}$, $\hat{k}=\hat{Z}$. Single equations can occur for the largest values of $|m|$.

The exponential operator connecting the pair of states $|m_a\rangle$ and $|m_b\rangle$ with $m_a=m_b+M$ can be expanded

$$\begin{aligned} e^{-i\xi(m_b)\tau} &= e^{-i\psi\tau}\{\cos q(m_b)\tau \\ &\quad - iq^{-1}(m_b)[\xi(m_b)-\psi]\sin q(m_b)\tau\} \\ &= e^{-i\psi\tau}[|m_a\rangle\langle m_a|f(m_b) - |m_a\rangle\langle m_b|g(m_b) \\ &\quad + |m_b\rangle\langle m_a|g^*(m_b) \\ &\quad + |m_b\rangle\langle m_b|f^*(m_b)], \end{aligned} \tag{14}$$

where

$$\begin{aligned} 2q(m_b) &= [\Delta^2(m_a m_b) + 4|v|^2(J_b 1 m_b M|J_a m_a)^2]^{1/2}, \\ f(m_b) &= \cos q(m_b)\tau - i[\Delta(m_a m_b)/2q(m_b)]\sin q(m_b)\tau, \\ g(m_b) &= i[v/q(m_b)](J_b 1 m_b M|J_a m_a)\sin q(m_b)\tau, \\ \Delta(m_a, m_b) &= \omega(m_a m_b) - \omega, \\ \psi(m_a, m_b) &= \tfrac{1}{2}\hbar^{-1}[E(m_a)+E(m_b)]. \end{aligned} \tag{15}$$

In these equations M takes on either the value of $M=0$, $M=+1$, or $M=-1$ for linear, left-circular, or right-circular polarization of the laser radiation. Again the notation $\omega(m_a m_b)=\hbar^{-1}[E(m_a)-E(m_b)]$ is used. The phase term $e^{-i\psi\tau}$ is only needed in problems in which a Stark or Zeeman splitting occurs.

B. Photon echoes

Let the first pulse occur during the interval t_0 to t_1 and the second pulse during the interval t_2 to t_3; these pulses are shown in Fig. 1. Also let the operators ξ_1 and ξ_2, which are defined by Eq. (8), with the appropriate value of the interaction V_I describe the first and second pulse and let $\xi_0 = H_0/\hbar$ describe the system between pulses. The unitary operator which describes the evolution of the molecular wave function is

$$\begin{aligned} U_\alpha(t,t_0) &= U_0(t,t_3)U_2(t_3,t_2)U_0(t_2,t_1)U_1(t_1,t_0) \\ &= e^{-i\xi_0(t-t_3)}A_2(t_3)e^{-i\xi_2(t_3-t_2)}A^\dagger(t_2) \\ &\quad\times e^{-i\xi_0(t_2-t_1)}A_1(t_1)e^{-i\xi_1(t_1-t_0)}A^\dagger(t_0). \end{aligned} \tag{16}$$

The subscript α indicates that the values of Δ_α, ω, v_α, φ_α, etc. which are appropriate for the αth molecule should be used.

The time dependence of the density matrix $\sigma(t)$ is given by

$$\sigma_\alpha(t) = U_\alpha(t,t_0)\sigma_\alpha(t_0)U_\alpha^\dagger(t,t_0), \tag{17}$$

and the electric dipole moment of the radiating molecule is

$$\begin{aligned} \vec{P}_\alpha &= \mathrm{Tr}\vec{P}\sigma_\alpha(t) \\ &= \sum_{m_b,m_a}\langle m_b|\vec{P}|m_a\rangle\langle m_a|\sigma_\alpha(t)|m_b\rangle + \text{c.c.} \end{aligned} \tag{18}$$

At time t_0 the states $|m_b'\rangle$ are equally probable if the molecule is in the lower state J_b and the states $|m_a'\rangle$ are equally probable if the molecule is in the upper state J_a. In the ensuing calculations the molecule is assumed in the state $|m_b'\rangle\langle m_b'|$ and then the average is taken over these equally probable states. Since

$$\sum\langle m_b|U|m_a'\rangle\langle m_a'|U^\dagger|m_a\rangle = -\sum\langle m_b|U|m_b'\rangle\langle m_b'|U^\dagger|m_a\rangle,$$

where the sum is over the repeated index, only the difference $\sigma_b-\sigma_a$ contributes to the electric dipole

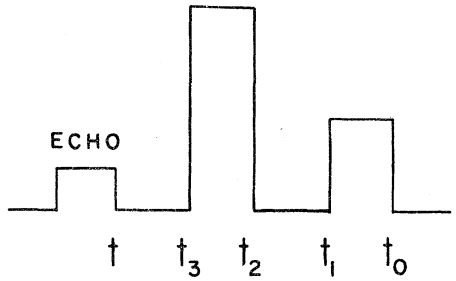

FIG. 1. Photon echo sequence. The first pulse begins at $t=t_0$ with duration t_1-t_0; the second pulse begins at $t=t_2$ with duration t_3-t_2; the echo occurs later at time t.

moment when $\sigma_b = \sigma(m_b')$ and $\sigma_a = \sigma(m_a')$, and it is sufficient to consider only the $|m_b'\rangle$ states.

Inspection of the $e^{-i\xi_0(t_3-t_2)}$ and $e^{-i\xi_0(t_2-t_1)}$ terms indicates that the only terms of the density matrix which contribute to the photon echo are

$$\begin{aligned}\langle m_a|\sigma(t)|m_b\rangle = [&\langle m_a|e^{-i\xi_2\tau_2}|m_b''\rangle\langle m_b''|e^{-i\xi_1\tau_1}|m_b'\rangle \\ &\times\langle m_b'|e^{i\xi_1\tau_1}|m_a''\rangle\langle m_a''|e^{i\xi_2\tau_2}|m_b\rangle \\ &\times e^{i[-\Delta t+\Delta_2 t_3+\Delta_2''t_2-\Delta_1''t_1]}] \\ &\times e^{i(2\varphi_2-\varphi_1)}e^{-i\omega t}+(\text{nonecho terms}),\end{aligned} \tag{19}$$

where $\Delta = \omega(m_a m_b) - \omega$, $\Delta_2'' = \omega(m_a'' m_b'') - \omega_2$, etc. If the first and second pulses have the same curvature, then $\varphi_2 = \varphi_1$, and the phase is the same as for the stimulating radiation. If the laser radiation does not change frequency between pulses, then $\omega_1 = \omega_2 = \omega$ and $\Delta = \Delta_1 = \Delta_2$. In the absence of Zeeman or Stark splitting and $\omega = \omega_1 = \omega_2$, $\Delta_\alpha(m_a m_b) = \Delta_\alpha = \omega_{ab} - \omega_\alpha$ and $\Delta = \Delta_1'' = \Delta_2'' = \Delta_2$, and the important phase term for photon echoes is

$$e^{-i\Delta[t-t_3-t_2+t_1]}.$$

As the average is taken over Δ_α, this term will be large near $t - t_3 = t_2 - t_1$.

Equation (19) includes greater detail than is often used for photon echoes. Yet this detail is necessary to evaluate the radius of curvature of the echo if the first and second pulses have different curvature[6] or directions. Also ω_1 and ω_2 are unequal in many experimental arrangements, and this decreases or eliminates the echo unless $\omega_1 = \omega_2$. $\Delta_i = \omega_{ab} - \omega(1 - \hat{k}\cdot\vec{v}_i/c)$ is the shift from velocity, and, as the average over velocity is taken in

$$\langle e^{-i\Delta(t-t_3-t_2+t_1)}e^{-i(\Delta-\Delta_2)(t_3+t_2)}e^{-i(\Delta-\Delta_1)t_1}\rangle,$$

a small change in velocity between the second pulse and the echo $(\Delta - \Delta_2)$ can cause an apparent relaxation time[7] as $t_3 + t_2$ is changed.

C. Linearly polarized pulses

Let the polarization of the first pulse $\hat{u}_1$ be along the $\hat{z}$ axis and the polarization of the second pulse $\hat{u}_2$ be along the $\hat{Z}$ axis for laser radiation which is along the $\hat{Y}$ direction. A rotation by angle β about the Y axis rotates the $\hat{Z}$ axis into the $\hat{z}$ axis, as shown in Fig. 2. The ξ_1 operator reduces to $m_a' = m_b'$ pairs, with z as the axis of quantization, and the ξ_2 operator reduces to $m_a = m_b''$ or $m_b = m_a''$ pairs with Z as the axis of quantization, and ξ_0 in the absence of Stark or Zeeman fields is diagonal in either representation. The equally probable initial states $|m_b'\rangle$ can be selected in either representation. It seems convenient to use the Z axis of quantization or the direction of the linear polarization of the second pulse as the primary axis. Thus the matrix element involving ξ_1 is evaluated by replacing $e^{-i\xi_1\tau}$ by the operator rotated through the angle β or by $e^{-i\beta J_Y}e^{-i\xi_1\tau}e^{i\beta J_Y}$. Then the matrix element of interest can be written

$$\begin{aligned}&\langle m_b''|e^{-i\xi_1\tau_1}\sigma(t_0)e^{i\xi_1\tau_1}|m_a''\rangle \\ &\quad = -\sigma_b\sum_{m_b'} r^{J_b}_{m_b'' m_b'} r^{J_a}_{m_a'' m_a'} f^*(m_b')g^*(m_b'),\end{aligned} \tag{20}$$

where $m_b' = m_a'$. The addition properties for rotation matrices[8] can be used to simplify this expression, and

$$\begin{aligned}r^{J_a}_{m_a'' m_a'} r^{J_b}_{m_b'' m_b'} = (-)^{m_b''-m_b'}\sum_J &(J_a J_b m_a'' - m_b''|JM) \\ &\times(J_a J_b m_a' - m_b'|J0)r^J_{M0}(\beta),\end{aligned} \tag{21}$$

where the sum over the integer values of J is from $|J_a - J_b|$ to $J_a + J_b$. Further simplification is obtained by interchanging the order of the J values in the C-G coefficients. The average electric dipole moment $\vec{P}_\alpha$ of the molecule at position $\vec{r}_\alpha$ is given by

$$\begin{aligned}\vec{P}_\alpha = \sum_{\substack{m_b, m_b' \\ J, M}} &G^*\hat{e}_M r^J_{-M0}(J_b 1 m_b M|J_a m_a) \\ &\times(J_b J m_a - M|J_a m_b)(J_b J m_b' 0|J_a m_a') \\ &\times\langle g_2(m_b+M)f_1^*(m_b')g_1^*(m_b')g_2(m_b) \\ &\times e^{-i\Delta(t-t_3-t_2+t_1)}\rangle + \text{c.c.},\end{aligned} \tag{22}$$

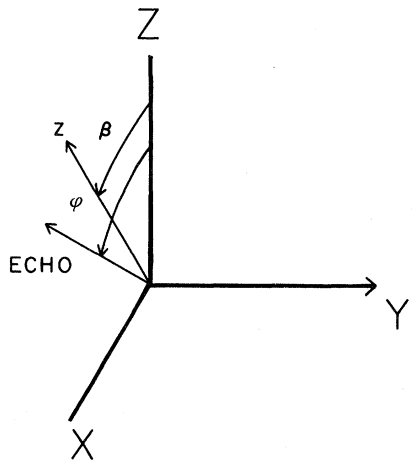

FIG. 2. Relative polarizations for pulses propagating along the Y axis. The linear polarization of the first pulse is along the z axis at an angle β to the linear polarization of the second pulse, which is along the Z axis. The linear polarization of the echo occurs at an angle φ from the Z axis.

where

$$G^* = e^{i(\varphi_\alpha - \omega t)}(\sigma_b - \sigma_a)(J_a \| P \| J_b)^* (2J_a+1)^{-1/2} \times [(2J+1)/(2J_a+1)]. \quad (23)$$

The rotation matrix is a function of the angle β, the $\hat{e}_M$ are the spherical basis unit vectors, and the values of $M = 0, \pm 1$.

The dependence of the electric dipole moment on the pulse strength v_α, the nearness to resonance Δ_α, and the pulse duration $\tau_1 = t_1 - t_0$ or $\tau_2 = t_3 - t_2$ is contained in the terms within the brackets $\langle\ \rangle$ which denote the thermal average. The properties of the first pulse are contained in the product $f_1^*(m_b')g_1^*(m_b')$, and a $\frac{1}{2}\pi$ first pulse occurs for

$$|(J_b 1 m_b 0 | J_a m_a) 2 v_1 \tau_1| = \tfrac{1}{2}\pi .$$

The second pulse depends on the terms $g_2(m_b+M)g_2(m_b)$ and a π second pulse occurs for $v_2\tau_2 = 2v_1\tau_1$. For $J_a = 1$ and $J_b = 0$ the maximum echo occurs for a $\frac{1}{2}\pi$ first pulse and a π second pulse. For larger values of J_a and J_b no single value of $v_1\tau_1$ will yield a $\frac{1}{2}\pi$ pulse for all transitions. Exact solutions are available for $J_a < \frac{7}{2}$ for arbitrary polarization of the first and second pulses. For large values of J_a and J_b which occur in molecular systems, i.e., $J_a = 20$–100, there is usually a group of states about a particular value of $|m_b|$ which yields values near $\frac{1}{2}\pi$ and π pulses. This feature becomes apparent by noting that the Clebsch-Gordon coefficients[9] of interest are

$$(J_b 1 m\, 0 | J_a m) = m/[J_b(J_b+1)]^{1/2} \quad \text{for } J_a = J_b$$
$$= -[(J_b - m)(J_b + m)/J_b(2J_b+1)]^{1/2} \quad \text{for } J_a = J_b - 1$$
$$= [(J_a - m)(J_a + m)/(2J_b+1)(J_b+1)]^{1/2} \quad \text{for } J_a = J_b + 1,$$

and therefore change slowly with m for large J_a and J_b. If the term with the largest C-G coefficient forms $\frac{1}{2}\pi$ and π pulses, then all other terms have weaker pulses, and the signs of the sine and cosine functions remain the same as the sums are taken over m_b and and m_b', and the electric dipole moment is appreciable. For larger values of $v_1\tau_1$ and $v_2\tau_2$ the sine and cosine functions can change sign, and cancellation can occur as the sum over m_b and m_b' is taken. In most experimental arrangements v_1 decreases as the laser radiation passes through the cell, and usually some region allows $v_1\tau_1$ to have the correct value for $\frac{1}{2}\pi$ pulses when the initial value of v_1 is near the correct value. If $v_1\tau_1$ is so weak that no pulse is stronger than $\frac{1}{6}\pi$, then the average tends to cancel and no echo occurs.

The angular dependence of P_X and P_Z on the angle β between the first and second pulses is contained in the dependence on the rotation matrices $r_{00}^J(\beta)$ and $r_{10}^J(\beta)$. P_Z depends on r_{00}^J, which is the Legendre polynomial $P_J(\cos\beta)$ and is a power series in $\cos\beta$. The angular dependence of P_X depends upon r_{10}^J, which may be obtained from the associated Legendre polynomials or from $r_{10}^J = [J(J+1)]^{-1/2}(d/d\beta)[P_J(\cos\beta)]$. If in Eq. (22) for P_Z or for P_X the terms for $-m_b'$ are combined with the terms for $+m_b'$ and the sign properties of the C-G coefficients are introduced, one can show that for $m_b' \neq 0$ only *odd* values of J occur. If $m_b' = 0$ occurs, then even values of J occur for this term when $J_a = J_b \pm 1$. Since this is only one term out of many for large J_a, to a good degree of approximation only odd values of J are important. One can use the relationship

$$(J_a J_b m_a m_b | JM) = (-)^{J_b + m_b}[(2J+1)/(2J_a+1)]^{1/2} \times (J_b J - m_b M | J_a m_a)$$

and the orthogonality condition[8]

$$\sum_{m_b} (J_a J_b m_a m_b | 1M)(J_a J_b m_a m_b | JM) = \delta_{J1} \quad (24)$$

to illustrate that there is cancellation in the full sum unless $J = 1$. Examination of the C-G coefficients for $J > 1$ indicates that the cancellation is due to the $(-)^m$ factor, and cancellation is expected when only part of the m_b' values are used. One of the C-G coefficients occurs in $g_1^*(m_b')$. Thus to a good approximation for large values of J_a the angular dependence of P_Z is given by $r_{00}^{(1)} = \cos\beta$ and P_X by $r_{10}^{(1)} = 2^{-1/2}\sin\beta$. There is no appreciable fine structure which depends on higher harmonics of $\cos\beta$ and $\sin\beta$.

Further examination of Eq. (22) indicates that P_Z and P_X differ by M in the C-G coefficients and in $g_2(m_b+M)$, and this is illustrated by the dashed lines in Fig. 3, which indicate the states which are connected by the C-G coefficients. The C-G coefficients for slant lines and vertical lines are in the ratio

$$(J_b 1 m_b 1 | J_a m_a)(J_b 1 m_a - 1 | J_a m_b)/(J_b 1 m_b 0 | J_a m_a)^2 ,$$

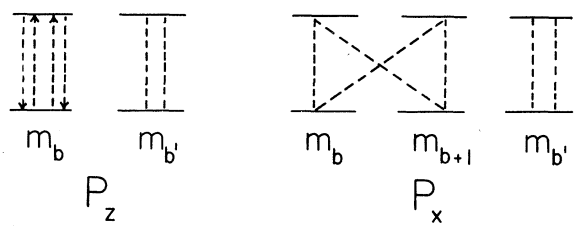

FIG. 3. Clebsch-Gordon coefficients which occur in Eq. (22) and which contribute to P_Z and P_X are shown by the dashed vertical and slanted lines.

which is approximately $\frac{1}{2}$ for $J_a = J_b \pm 1$ and $(J_a^2 - m_a^2)/2m_a^2$ for $J_a = J_b$. Since P_X is summed over $M = \pm 1$, this contribution is approximately equal to P_Z for $J_a = J_b \pm 1$ and is pulse-strength sensitive for $J_a = J_b$. The primary differences between P_Z and P_X are the $2^{-1/2}$ in the coefficient, the $2^{-1/2}$ from $r_{10}^{(1)}$, and the sign dependence of the C-G coefficients. If only these primary differences are taken into consideration, the electric polarization of the photon echo from molecules with large values of J_a is approximately proportional to

$$\vec{P} \propto [\mp \hat{X}(\tfrac{1}{2}\sin\beta) + \hat{Z}\cos\beta], \tag{25}$$

where the plus sign refers to $J_a = J_b$ or to the Q-branch transition and the negative sign to the $J_a = J_b \pm 1$ or to the P- and R-branch transitions. The photon echo is linearly polarized at an angle φ from the $\hat{Z}$ axis, as shown in Fig. 2, and is given by

$$\tan\varphi = P_X/P_Z \simeq \pm\tfrac{1}{2}\tan\beta\,. \tag{26}$$

For $J_a = J_b \pm 1$ or the P and R branch transitions the echo polarization rotates in the opposite sense of β and for $J_a = J_b$, or for Q-branch transitions the echo polarization rotates in the same sense as β. This sense of rotation is apparent in the earlier developments[2,3] for the $J_a = 2 \rightarrow J_b = 1$ and the $J_a = 2 \rightarrow J_b = 2$ transitions. The $\frac{1}{2}$ in Eqs. (26) and (27) is an excellent approximation for the $J_a = J_b \pm 1$ transitions and is a good approximation for $J_a = J_b$ if the strength of the pulses favors the $m_b' = 2^{-1/2} J_b$ states. The intensities of the X and Z components of the echo are given by

$$I_X \simeq \tfrac{1}{4} I_0 \sin^2\beta\,, \quad I_Z \simeq I_0 \cos^2\beta\,. \tag{27}$$

At $\varphi = +45°$ or at $\beta = 63.4°$ the intensities are approximately equal.

Although it has not been emphasized, it should be noted that the phase is preserved in Eq. (22), and the radiation generated by the assembly of electric dipole moments has the same phase as the stimulating laser radiation.[6]

It has been noted in the discussion that the theory applies to either $J_a = J_b \pm 1$ and the $J_a = J_b$ atomic[10] lines or to the corresponding P, R and Q branches of the molecular lines. The Wigner-Eckart theorem has been used for the matrix elements of the electric dipole P_M. The matrix elements for this operator for the symmetric top is readily evaluated by transforming to the body-fixed frame P_k, $P_M = R_{Mk}^{*(1)}(\alpha, \beta, \gamma) P_k$, and by noting that the symmetric-top wave functions are related to the rotation operator[11] by $\psi(KJm) = [(2J+1)/8\pi^2]^{1/2} R_{mK}^{*(J)}(\alpha, \beta, \gamma)$. Direct evaluation yields

$$(vKJm|P_M|v'K'J'm') = C_k (J'1m'M|Jm) \times (J'1K'k|JK), \tag{28}$$

where $C_k = (v\|P_k\|v')[(2J'+1)/(2J+1)]^{1/2}$. The index v denotes the vibrational coordinates, and a sum over the repeated index k is implied. For a vibration rotation transition for a symmetric-top molecule $C_\pm = 0$ for a vibration along the symmetry axis and $C_0 = 0$ for a transverse vibration, and the selection rule for K is $\Delta K = 0, \pm 1$ for an electric-dipole transition. The dependence on Jm is the same as for atoms, and the reduced matrix element v_α in Eq. (13) and G^* in Eq. (23) is replaced by $C_k(J'1K'k|JK)$. A sum is needed for all K values which are excited by the laser pulses.

The spherical-top molecules SF_6 and SiF_4[12] are of particular interest. The ν_3 vibrational band has a three-fold degeneracy, and there is a Coriolis interaction in the first excited state of the ν_3 band with the total angular momentum $\vec{J}$. If the ν_3 vibrational-state wave function $|v_a v_b v_c)$ is written as $|vY_{lm_l}^*)$, where v is the vibrational quantum number 0 or 1 and $Y_{lm_l}^*$ is the spherical harmonic which describes the vibrational angular momentum, the Coriolis interaction[13] in the rotational Hamiltonian $H_r = BJ^2 - 2B\zeta_3(\vec{l}\cdot\vec{J})$ can be diagonalized in the representation which couples K and m_l. If the angular momentum G is defined as $\vec{J} = \vec{G} + \vec{l}$, the appropriate wave function is

$$|vlGm_G Jm) = \sum_{Km_l} |KJm)|vY_{lm_l}^*)(Jl Km_l|Gm_G)\,. \tag{29a}$$

The Coriolis interaction splits the $l = 1$ level into a triplet with $G = J+1, J, J-1$. With $v = 1$, $l = 1$ and $v' = 0$, $l' = 0$ the matrix element of the electric dipole operator is

$$(11Gm_G Jm|P_M|00J'K'J'm') = C\delta_{GJ'}\delta_{K'm_G} \times (J'1m'M|Jm)\,. \tag{29b}$$

This matrix element selects out the transition with $m_G = K'$ and $G = J'$, where K' and J' are the quantum numbers of the $v' = 0$ or lower vibrational level. $G = J' = J-1, J, J+1$ yields the P, Q, and R branches, and the transition frequencies[13] are $\nu_P = \nu_0 - 2B(1-\zeta_3)J$, $\nu_Q = \nu_0$, and $\nu_R = \nu_0 + 2B(1-\zeta_3) \times (J+1)$. Second-order Coriolis interactions can split the levels of interest into $2m_G + 1 = 2J' + 1$ levels. Since $C = 3^{-1/2}(1\|P\|0)$, the electric-dipole matrix element is independent of K, and the reduced matrix element for v_α in Eq. (13) and G^* in Eq. (23) is similar to the atomic case. If the laser transition can excite more than one K state, a sum is needed over these states.

III. EXPERIMENTAL PROCEDURE

The experimental apparatus used to investigate the polarization of photon echoes from SF_6 is

shown in Fig. 4. It is similar to apparatus used in earlier echo experiments.[2,5] The two CO_2 lasers which generate the two exciting pulses were both Q switched by a common rotating mirror RM which was gold coated on both sides. The rotating mirror was symmetrically positioned between intracavity reflection gratings G located at the ends of both discharge tubes. Rotation of each grating about the vertical axis permitted the selection of a specific laser frequency, while rotation of each grating about the horizontal axis varied the pulse separation from +10 μsec to −10 μsec between the two lasers pulses. Both lasers were made to operate in the TEM_{00} mode by the use of beam-limiting apertures. Typical pulse duration was 300 nsec, with a repetition rate of 100 Hz.

The output intensities were controlled by ethyl-ether absorption cells EC. These cells were used to reduce the pulse intensity and to adjust the intensity ratio of the first pulse to the second pulse to 1 to 4. The two beams were made coincident and collinear with a dielectric coated Ge beam splitter. A 10-m radius-of-curvature mirror collimated the two beams through the 6-m SF_6 sample cell. After passing through the sample cell, the pulses were focused onto the input window of a Cu:Ge detector. Output from the detector was displayed on a Tektronix 547 oscilloscope.

The output pulses from both lasers were linearly polarized by the Brewster angle windows on the discharge tubes. In order to vary the plane of polarization of one laser pulse with respect to the other, the output from one laser passed through a CdS quarter-wave plate and a grid polarizer P_1.

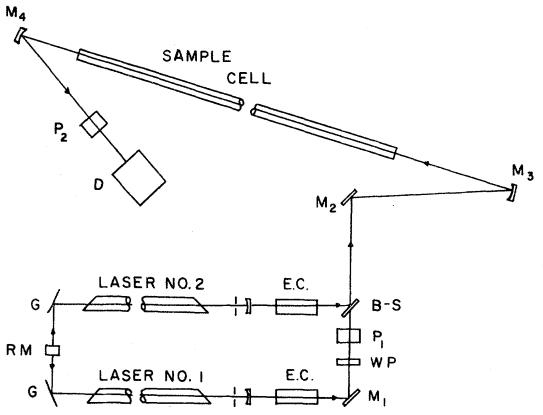

FIG. 4. Experimental apparatus. Rotating mirror Q-switch: RM; intra-cavity reflection grating: G; ether cell: EC; flat mirrors, gold coated: M_1 and M_2; focusing mirror with 10-m radius of curvature, aluminum coated: M_3; focusing mirror with 2-m radius of curvature, aluminum coated: M_4; CdS wave plate: WP; grid polarizers: P_1 and P_2; dielectric coated Ge beam splitter: B-S; Cu-Ge photoconductor: D.

A second grid P_2 was used to analyze the polarization of the pulses coming from the sample cell. This analyzer was positioned just before the detector. Both polarizer and analyzer were constructed by using the method of Bird and Parrish.[14] Aluminum was evaporated at a grazing angle onto two thin-film first-generation plastic replicas with 1800 lines per millimeter. Gold was then evaporated over the aluminum at the same grazing angle to retard oxidation of the aluminum. This technique produced polarizers with 95% efficiency. There is probably no advantage to using an initial aluminum coating.

This apparatus was used to measure the polarization of photon echoes from SF_6 which were stimulated by the $P(14)$, $P(16)$, $P(18)$, $P(20)$, $P(22)$, and $P(24)$ CO_2 laser lines near 10.6 μm. For each line the input pulse intensities were adjusted to give a maximum echo signal, and these intensities were in agreement with earlier measurements.[5] SF_6 pressures of a few milliTorr were made with a McCleod gauge.

IV. EXPERIMENTAL RESULTS

The experimental results are given in Secs. IV A, IV B, and IV C for the linear-linear, circular-linear, and linear-circular pulse sequences. Since stimulation with the $P(16)$ laser line of CO_2 yields an echo polarization which is distinctly different from that stimulated by the $P(14)$, $P(18)$, $P(20)$, $P(22)$, and $P(24)$ lines, $P(16)$ is discussed separately.

A. Linear-linear

1. P(16)

The SF_6 transition which is stimulated by the $P(16)$ line of CO_2 at 10.551 μm provides a strong echo which has both X and Z intensity components. The relative echo intensities I_Z and I_X are shown in Fig. 5 as a function of the angle β, and the sense of β is shown in Fig. 2. The second pulse is linearly polarized along $\hat{Z}$, and the first pulse is linearly polarized along $\hat{z}$ at angle β to $\hat{Z}$. I_Z is proportional to $\cos^2\beta$, and I_X is proportional to $\sin^2\beta$, and this angular dependence of the intensity is in accord with Eq. (27). The intensities are approximately equal at $\beta = 63°$, but the amplitude of I_K at $\beta = 90°$ is approximately 0.3 and is somewhat larger than the 0.25 suggested by Eq. (27). The echo is linearly polarized at an angle φ with the linear polarization $\hat{Z}$ of the second pulse, and the angle φ as a function of the angle β is shown in Fig. 6. Since the echo angle φ rotates in the same sense as β, the theory which lead to Eq. (26) allows the conclusion that this photon echo is produced by a $J_a = J_b$ transition or by the Q branch of the SF_6

molecule. It is also apparent from Fig. 6 that the angle dependence is in reasonable agreement with Eq. (26). Since the Q branch is saturation sensitive, it would appear that the $\frac{1}{2}$ term in Eqs. (25) and (26) is a good approximation for a typical experimental arrangement.

The decay of the echo amplitude with the time interval $t_2 - t_1 = \tau$ between pulses permits the determination of a relaxation rate T_2^{-1} for the destruction of the photon echo. T_2^{-1} is determined from a plot of echo intensity versus the time interval $2(t - t_0) \simeq 4\tau$ or $\ln(I/I_0) \simeq -4\tau/T_2$, and is shown as a function of pressure in mTorr in Fig. 7 for the I_Z and I_X components of the polarization. The I_Z component exceeds noise at a pressure of 6 mTorr, and this component of the echo is a maximum at approximately 2.3 mTorr. The I_X component exceeds noise at a pressure of 3 mTorr and is also a maximum at 2.3 mTorr. The relaxation rate T_2^{-1} for the two components is

$$PT_{2X} = 4.6\,\text{nsec Torr}, \quad PT_{2Z} = 5.4\,\text{nsec Torr}.$$

The signal-to-noise ratio should be improved before speculating in to great detail on the difference in these relaxation rates. With the assumption that $T_2^{-1} = n\langle V\sigma\rangle$, this relaxation rate yields the rather large cross section of $\sigma \simeq 2100 \times 10^{-20}$ m^2 for the destruction the photon echo.

2. P(14), P(18), P(20), P(22), P(24)

The I_Z component of the intensity is shown in Fig. 8 for the photon echoes from SF_6 molecules stimulated by the $P(14)$, $P(18)$, $P(20)$, $P(22)$, and $P(24)$ lines of CO_2 near 10.5 μm. The data for each line falls within the error bars shown in the figure, and for each of these lines $I_Z/I_0 \simeq \cos^2\beta$. This is in accord with the theory for large J_a values which is given by Eq. (27). No X component of the intensity, $I_X = 0$, was observed for any of these lines. A signal which was 0.1 I_X for $P(16)$ or 0.05 I_Z for these lines could have been observed. This data indicates that I_X is much smaller than the value given by Eq. (27).

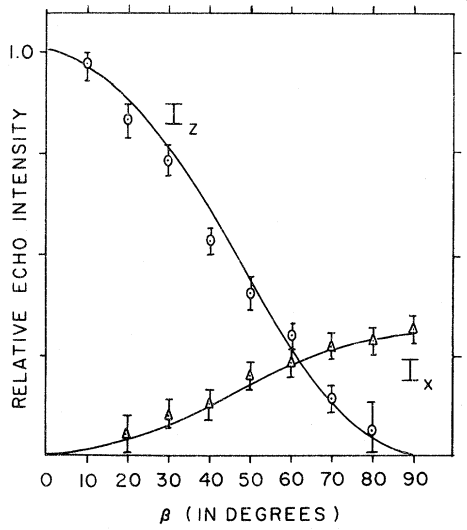

FIG. 5. Relative photon-echo intensity as a function of β for SF_6 molecules stimulated by the $P(16)$ line of CO_2. Curves are shown for $I_Z/I_0 = \cos^2\beta$ and $I_X/I_0 = 0.3\,\sin^2\beta$.

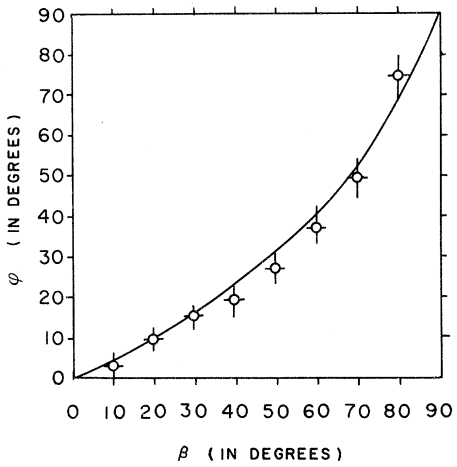

FIG. 6. Angle φ of the linear polarization of the photon echo which is shown in Fig. 5 as a function of the angle β. The curve follows $\tan\varphi = \frac{1}{2}\tan\beta$ and should be compared with Eq. (26).

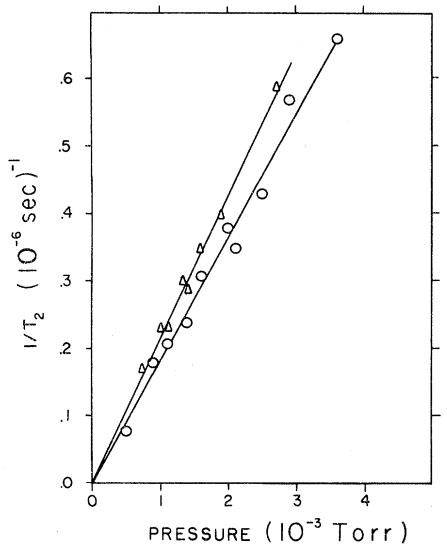

FIG. 7. Relaxation rate T_2^{-1} as a function of SF_6 pressure in mTorr. Triangles represent data for X component of the echo, and circles represent data for Z component of the echo. Data taken on $P(16)$ for a linear-linear sequence.

B. Circular-linear

1. P(16)

The optimum echo stimulated by a left-circularly polarized first pulse and a linearly polarized second pulse occurred when the intensity ratio was 1 : 2 and the intensity of the first pulse was approximately 0.1 W/cm^2. A CdS quarter-wave plate was used to produce the circularly polarized pulse. The output was analyzed with the grid analyzer, and the intensity as a function of angle α between the grid analyzer and the Z axis of the linearly polarizer second pulse is shown in Fig. 9. The intensity is approximately given by

$$I/I_0 \simeq 0.3 \sin^2\alpha + \cos^2\alpha$$

and indicates elliptic polarization. In order to determine the sense of the elliptic polarization a CdS quarter-wave plate was positioned just before the grid analyzer. The circularly polarized first pulse was linearly polarized by the wave plate. As the grid analyzer was rotated to block the first pulse, the echo intensity was maximized. Alternatively, when the analyzer was rotated for maximum transmission of the first pulse, the echo vanished. These results indicate that a *left*-circular first pulse produced a *right* elliptic echo. This can be combined with the intensity data in Fig. 9 to yield an echo polarization vector of approximately $-\frac{1}{2}i\hat{X}+\hat{Z}$ and is in good agreement with Eq. (A2). This data and Eq. (A2) imply that this is a Q-branch transition and are in accord with the linear-linear result. The best intensity ratio of 1 : 2 is also suggested by Eq. (A1) for the Q branch. The X component disappeared into the noise at an intensity ratio of 1 : 4, and a weak X component reappeared at a ratio of 1 : 8.

2. P(14), P(18), P(20),

The echo stimulated by these three lines was optimum for an intensity ratio of 1 : 8 and a first pulse intensity of 0.2 W/cm^2. The echo was linearly polarized along the linear polarization of the second pulse. There was no X component of the echo polarization. The optimum intensity ratio suggests a P or R branch. Since the terms in Eq. (A1) which yield $\frac{1}{2}i\hat{X}$ in Eq. (A2) are similar to those in Eq. (22) which yield $-\frac{1}{2}\hat{X}$ in Eq. (25), the absence of this term for the circular-linear sequence is consistent with the absence of the similar term for the linear-linear sequence.

C. Linear-circular

P(14), P(16), P(18), P(20)

The photon echoes stimulated by a linearly polarized first pulse and a *left*-circularly polarized second pulse were *left*-circularly polarized. This result is in accord with Eq. (A4), which indicates that for large values of angular momentum J_a the echo has the same circular polarization as the second pulse for either the P, Q, or R branches. The echo intensity was not particularly sensitive to the intensity ratio, and good echoes were observed at ratios of 1 : 2, 1 : 4, and 1 : 8.

V. DISCUSSION OF RESULTS

The echo polarization for large and small values of total angular momentum J_a is given by Eq. (22) for linearly polarized first and second pulses and

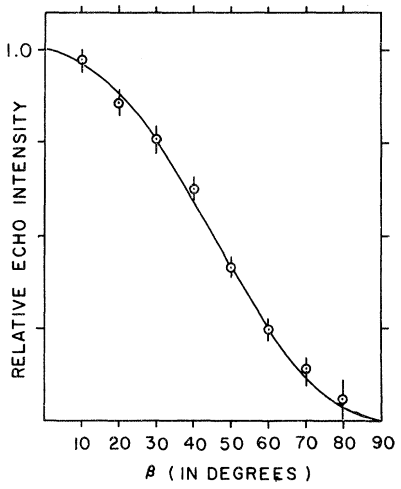

FIG. 8. Relative echo intensity I_Z/I_0 as a function of β, the angle between the polarizations of the exciting pulses. Error bars include data for $P(14)$, $P(18)$, $P(20)$, $P(22)$, and $P(24)$. $I_X \simeq 0$ for all lines.

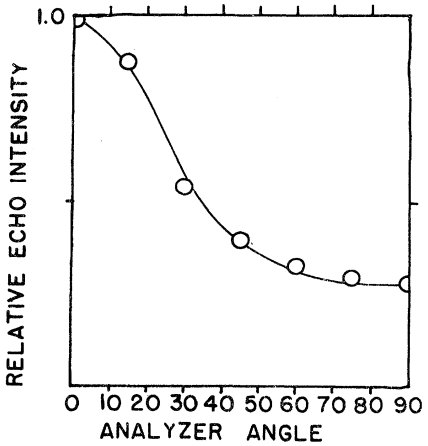

FIG. 9. Relative echo intensity for stimulation by a circularly polarized first pulse and a linearly polarized second pulse with $P(16)$ as a function of analyzer angle α. The curve is drawn for $I/I_0 = 0.3 \sin^2\alpha + \cos^2\alpha$.

in the Appendix for circular-linear and linear-circular sequences. For large values of J_a this expression would involve thousands of terms. Fortunately, for these large values the echo polarization can be approximated in the simple form of Eqs. (25), (A2), or (A4).

Equation (25) provides a good approximation for the echo polarization in terms of the angle β between the linearly polarized first and second pulses. The echo is linearly polarized at an angle φ, with the linear polarization of the second pulse, and φ rotates in the same sense as β for $J_a = J_b$ or for the Q branch. φ rotates in the opposite sense of β for $J_a = J_b \pm 1$ or for the P- and R-branch molecular transitions. This sense of rotation is in agreement with the comments in the paper of Gordon *et al.*, but is in the opposite sense to the curves which are shown in Figs. 8 and 9 of their paper. Except for a sign error, the curves for $J = 5$ in their paper have the same angular features as Eq. (25) for large J. Equation (25) considers selective excitation of a group of m states, and the amplitude of the X component of the echo is smaller than that suggested by Gordon *et al.* for the Q branch. Thus the intensity ratio at $\beta = 90°$ and $\beta = 0$ is $I(90)/I(0) \simeq 0.4$ from their paper for pulses of short duration for the Q branch, and for $J = 5$ for the P and R branches $I(90)/I(0) \simeq 0.2$. This paper suggests that $I(90)/I(0) \simeq 0.25$, is probably a better approximation for the P, Q, and R branches when a limited group of m values are important.

For a *left*-circularly polarized first pulse and a linearly polarized second pulse Eq. (A2) indicates that P and R branches or $J_a = J_b \pm 1$ have *left* elliptic polarization and that the Q or $J_a = J_b$ transition has *right* elliptic polarization. Furthermore, the best intensity ratio for $\frac{1}{2}\pi$ and π pulses is no longer 1 : 4, but is 1 : 2 for the Q branch and 1 : 8 for the P and R branches. These intensity ratios are estimated by examining the terms in Eq. (A1).

For a linearly polarized first pulse and a left-circularly polarized second pulse for large J_a Eq. (A4) indicates that the echo has left-circular polarization. The best intensity ratios for the production of echoes is estimated to be 1 : 8 for the Q branch and 1 : 2 for the P and R branches.

Only the echo which is stimulated in SF_6 by the $P(16)$ line of a CO_2 laser is in good agreement with the theory which is given in this paper. The echo is linearly polarized at an angle φ, with the linear polarization of the second pulse and rotates in the same sense as the angle β between the first and second pulses. For a left-circularly polarized first pulse and a linearly polarized second pulse the echo has right elliptic polarization. Both of these unusual features are given by the theory for the Q branch for large values of J_a. For a linear-linear sequence an intensity ratio of 1 : 4 provides good echoes and for a circular-linear 1 : 2 provides good echoes, and again this characteristic of a Q branch-transition. The maximum amplitude of the X component is approximately one-half of the amplitude of the Z component and is in accord with the simple approximations which were used for Eqs. (25) and (A2). Gibbs and Salamo[15] in their discussion of self-induced transparency pulse breakup in SF_6 consider this as a Q-band transition.

The experimental results for the echoes stimulated by the $P(14)$, $P(18)$, $P(20)$, $P(22)$, and $P(24)$ CO_2 laser lines obeyed the equations $I_Z = I_0 \cos^2\beta$ and $I_X = 0$ within the experimental accuracy for the linear-linear sequence. A similar result was observed by Gordon *et al.* in the initial SF_6 echo polarization measurement with $P(20)$. This result is expected for a $J_a = 1 \rightarrow J_b = 0$ transition, but these small J values are quite improbable.[4] For a circularly polarized first pulse and a linearly polarized second pulse the echo from these transitions is always linearly polarized along the second pulse. For a linearly polarized first pulse and a left-circularly polarized second pulse, the echo is left-circularly polarized for all of these transitions, and only this sequence is in good agreement with the theory.

A simple explanation for the absence of a P_X echo component of electric polarization stimulated by linear-linear or circular-linear pulses of these lines would be to argue that they are formed by a superposition of contributions from the P and Q or Q and R branches. Brunet and Perez[16] examined the ν_3 and ν_4 absorption bands of SF_6. Although the P, Q, and R branches of the ν_3 band near 10.6 μm could not be resolved, these branches could be resolved for the ν_4 band near 16.3 μm, and a value of the Coriolis constant $\zeta_4 = -0.24$ was reported. The Q branch was broad, and they suggested that this breadth was due to transitions which started from the thermally excited ν_6 levels or hot-band transitions. Using the ζ sum rule they suggested a value of $\zeta_3 = 0.73$. If the hot band or ν_6 contribution to the Q branch of the ν_3 vibration-rotation transition is similar to that for ν_4, and the width of the P and R branches are reduced by a factor of $(1 - \zeta_3)/(1 - \zeta_4) \simeq \frac{1}{4}$, then the overlap of the P and Q and Q and R bands is appreciable. From this point of view the absorption data of Brunet and Perez could be interpreted as indicating appreciable overlap of the P and Q bands for the $P(22)$, $P(20)$, and $P(18)$ laser lines of CO_2 and between the Q and R branches for the $P(14)$ line. The $P(16)$ line could be almost pure Q branch. The high-resolution spectroscopy and Lamb dip spectroscopy of Shimizu[4] showed that absorption lines overlap

within the Doppler width, but that strong single lines also occur near the $P(12)$ through $P(18)$ transitions. Line spacings of 5–15 MHz were observed by Rabinowitz, Keller, and La Tourette[17] for many of these lines, and four lines were observed within the Doppler width for stimulation with $P(16)$ or $P(20)$. One line stimulated by $P(16)$ was very strong. All lines for $P(20)$ were regarded as weak or very weak. These line densities can be expected when the second-order Coriolis interaction lifts the K degeneracy and splits the spacing $\delta\nu_3 = 2B(1-\zeta_3) = 1.5$ GHz into $2J+1$ levels. For a pulse duration of 300 nsec and a Doppler width of 28 MHz in SF_6 all of the lines within the Doppler width contribute to the echo. Although the cancellation of the P_X component by the overlap of the P and Q or Q and R branches appears possible, this conclusion must be regarded as quite speculative.

It may be noted from Eq. (29a) that the effective electric dipole moment of the spherical-top molecule for a ν_3 vibration rotation transition is proportional to the C-G coefficient $(J'lm'M|Jm)$ and its magnitude[9] changes only with ΔJ and Δm. The pulse strengths reported by Meckley and Heer for optimum echoes suggested a change in effective electric dipole moment of as much as 3 : 1 between the $P(18)$ and $P(24)$ excitation. These changes are larger than expected, but could be accounted for by taking into consideration the degree of off resonance when multiple lines occur within the excitation width. Direct absorption experiments which resolve single lines have the same line strength for all lines and should be sensitive only to the number of molecules thermally excited to a given state. The absorption data of Shimizu[4] is consistent with this conclusion.

Zembrod and Gruhl[18] have observed pulse break up in SF_6 for self-induced transparency for excitation by the $P(12)$, $P(14)$, $P(16)$,, and $P(20)$ lines. The break up and transmission of $P(12)$ and $P(14)$ were distinctly different from $P(16)$ and $P(20)$. Since it was felt that degeneracy and the different electric dipole moments for these degenerate levels was important in the explanation of these differences, Salamo, Gibbs, and Churchill[19] studied self-induced transparency for Na atoms excited with a dye laser. For these low values of angular momentum, $F=2$ and 1, the pulse shape for these degenerate levels with different transition dipole moments was in agreement with theory. For short pulses which excited more than one state and for which the transition dipole moments were equal, the results were in agreement with the nondegenerate or two-level-atom example.[20] For the large values of J which occur in SF_6, the theory of Rhodes and Szoke[21] is needed for the distribution of dipole moments. Zembrod and Gruhl interpret their $P(16)$ data in agreement with a large degeneracy, but the $P(12)$ and $P(14)$ have features of nondegenerate levels, and they use a theory of strong relaxation coupling[22] to remove the degeneracy. This later assumption would also destroy the slant terms in Fig. 3 and destroy P_X for these levels. Some care is necessary since the dipole moment depends on $(m^2/J^2)^{1/2}$ for the Q branch and on $[(J^2-m^2)/2J^2]^{1/2}$ for the P and R branches, and there is a tendency for the P and R branches to have an effective moment near the $m=0$ value and appear more nearly nondegenerate. If the R and Q branches overlap for $P(14)$, then the superposition of these two quite different moments may assist in explaining their observations.

The six flourine atoms in SF_6 each have a nuclear spin of $I_i = \frac{1}{2}$. The 64 possible states with $m_I = \sum m_i$ can be divided into one with $I=3$, five $I=2$, nine $I=1$, and five $I=0$ nuclear momentum states. Since the over-all wave function must change sign under the exchange of two flourine atoms, a group-theory development is necessary to label the wave function of the various states. In the absence of appreciable splitting of the nuclear levels it would seem that Eq. (29b) for the matrix element remains correct with $I=I'$ and $m_I = m_I'$, and nuclear spin can be ignored. If for reasons which are not apparent there is a splitting of the order of 1 MHz and $\vec{F} = \vec{I} + \vec{J}$ is the appropriate quantum number, then the matrix element Eq. (29b) is replaced by

$$(11Gm_G IJFm|P_M|00J'K'I'J'F'm') = C\delta_{GJ'}\delta_{K'm_G}\delta_{II'}\begin{Bmatrix} JJ'1 \\ F'FI \end{Bmatrix}(F'1m'M|Fm).$$

The selection rules are $\Delta J = 0, \pm 1$ and $\Delta F = 0, \pm 1$. For large values of J the six-j coefficient is small unless $\Delta J = \Delta F$, and the discussion for zero nuclear spin remains correct. If J is of the order of I, then for either the P, Q, or R branch $\Delta F = 0, \pm 1$ and a sum over F is needed.[19] Since P_X has opposite sign for $\Delta F = 0$ and $\Delta F = \pm 1$, there is a tendency for cancellation.

Note added in proof. W. M. Gutman and C. V. Heer have informed us that recent measurements indicate that photon echoes which were stimulated by linear-linear, circular-linear, and linear-circular pulse sequences in SF_6 by the $P(14)$ laser line were in good agreement with the theory of this paper for an R branch transition.

APPENDIX

1. Circular-linear

If the first pulse is left-circularly polarized and the second pulse is linearly polarized the problem remains two level by choosing the axis of quantiza-

tion of the circular pulse along the direction of the laser radiation and the axis of quantization Z of the second pulse along the linear polarization. With XYZ as the reference axes and with the laser radiation along Y, the two sets of axes are related by a rotation by $\frac{1}{2}\pi$ about the Z axis followed by a $\frac{1}{2}\pi$ rotation about the new y' axis. The operator $e^{-i\xi_1\tau_1}$ is replaced by

$$e^{-iJ_Z\pi/2}e^{-iJ_Y\pi/2}e^{-i\xi_1\tau_1}e^{iJ_Y\pi/2}e^{iJ_Z\pi/2},$$

and with this transformation ξ_1 connects state m_b' with $m_a'=m_b'+1$ for left-circular polarization. Following the earlier procedure which was used to derive Eq. (22), the electric dipole moment of the stimulated molecule is given by

$$\vec{P}_\alpha=\sum_{\substack{m_b m_b' \\ JM}} G^*\hat{e}_M r^J_{-M1}\left(\frac{\pi}{2}\right)e^{-iM\pi/2}(J_b 1 m_b M|J_a m_a)(J_b J m_a - M|J_a m_b)(J_b J m_b' 1|J_a m_a')$$
$$\times\langle g_2(m_b+M)f_1^*(m_b')g_1^*(m_b')g_2(m_b)e^{-i\Delta(t-t_3-t_2+t_1)}\rangle + \text{complex conjugate}. \tag{A1}$$

Again the sum over m_b' suggests that orthogonality limits the important contributions to $J=1$ for large J_a. A comparison of the terms suggests that $\vec{P}$ is elliptically polarized with

$$\vec{P}\propto\pm\tfrac{1}{2}i\hat{X}+\hat{Z}, \tag{A2}$$

where the quantity within the brackets is the coefficient of $e^{-i\omega t}$. The positive sign refers to the P and R branches or $J_a=J_b\pm1$, and the echo has left elliptic polarization. The negative sign refers to the Q branch or $J_a=J_b$, and the echo has right elliptic polarization. Since the $\hat{X}$ component of the Q branch is saturation sensitive, the $\frac{1}{2}$ coefficient is an approximation and is similar in magnitude to the similar coefficient in Eq. (25). Since $\Delta m=1$ occurs in $f_1^*g_1^*$ and $\Delta m=0$ in g_2g_2, the best intensity ratio between the first and second pulse is no longer in the ratio 1 : 4. For the Q branch the ratio 1 : 2 may yield better echoes. For the P and R branches 1 : 8 may be appropriate.

2. Linear-circular

If the first pulse is linear and the second pulse is left circular, it is convenient to choose the axis of quantization Z along the direction of the laser radiation. The first pulse reduces to a two-level problem under a rotation of $\frac{1}{2}\pi$ about Y followed by a rotation of $\frac{1}{2}\pi$ about the new z' axis, and $e^{-i\xi_1\tau_1}$ is replaced by the transformed operator. The electric dipole moment is given by

$$\vec{P}_\alpha=\sum_{\substack{m_b m_b' \\ JM}} G^*\hat{e}_M r^J_{-M'0}\left(\frac{\pi}{2}\right)(J_b 1 m_b M|J_a m_a)(J_b J m_b'' - M'|J_a m_a'')(J_b J m_b' 0|J_a m_a')$$
$$\times\langle g_2(m_b'')f_1^*(m_b')g_1^*(m_b')g_2(m_b)e^{-i\Delta(t-t_3-t_2+t_1)}\rangle + \text{c.c.}, \tag{A3}$$

where $m_b''=m_a-1$ and $m_a''=m_b+1$. Again $J=1$ is the dominant term for large J_a. If only the $J=1$ term is kept the echo is left-circularly polarized, i.e., only the $M=1$ term is nonzero, or the coefficient of $e^{-i\omega t}$ is

$$\vec{P}\propto\hat{e}_+. \tag{A4}$$

For the P and R branches the best intensity ratio is probably 1 : 2 and for the Q branch 1 : 8.

[1] I. D. Abella, N. A. Kurnit, and S. R. Hartman, Phys. Rev. 141, 391 (1966).
[2] J. P. Gordon, C. H. Wang, C. K. N. Patel, R. E. Slusher, and W. J. Tomlinson, Phys. Rev. 179, 294 (1969).
[3] C. V. Heer and R. H. Kohl, Phys. Rev. A 1, 693 (1970).
[4] F. Shimizu, Appl. Phys. Lett. 14, 378 (1969).
[5] J. R. Meckley and C. V. Heer, Phys. Lett. 46A, 41 (1973).
[6] C. V. Heer, Phys. Rev. A 7, 1635 (1973).
[7] J. Schmidt, P. R. Berman, and R. G. Brewer, Phys. Rev. Lett. 31, 1103 (1973); C. V. Heer, Phys. Lett. 49A, 213 (1974); C. V. Heer, Phys. Rev. A 10, 2112 (1974).
[8] A. Messiah, *Quantum Mechanics* (North-Holland, Amsterdam, 1962), Appendix C, Vol. II.
[9] M. E. Rose, *Elementary Theory of Angular Momentum* (Wiley, New York, 1957), p. 225; E. U. Condon and G. H. Shortley, *The Theory of Atomic Spectra* (Cambridge U. P., London, 1957), p. 76.
[10] B. Bolger and J. C. Diels, Phys. Lett. 28A, 401 (1968).
[11] W. H. Shaffer and J. D. Louck, J. Mol. Spectrosc. 3, 123 (1959).
[12] J. Nella, Appl. Phys. Lett. 23, 568 (1973).
[13] W. H. Shaffer, H. H. Nielsen, and L. H. Thomas,

Phys. Rev. 56, 895 (1939). Less detailed references are given in W. F. Edgell and R. E. Moynihan, J. Chem. Phys. 27, 155 (1957); H. C. Allen, Jr., and P. C. Cross, *Molecular Vib-Rotors* (Wiley, New York, 1963); D. Steele, *Theory of Vibrational Spectroscopy* (Saunders, Philadelphia, 1971).

[14]G. Bird and M. Parrish, J. Opt. Soc. Am. 50, 886 (1960).

[15]H. M. Gibbs and G. J. Salamo, in *1974 International Quantum Electronics Conference Digest of Technical Papers* (IEEE, New York, 1974), p. 66.

[16]H. Brunet and M. Perez, J. Mol. Spectrosc. 29, 472 (1969).

[17]P. Rabinowitz, R. Keller, and J. T. LaTourette, Appl. Phys. Lett. 14, 376 (1969).

[18]A. Zembrod and Th. Gruhl, Phys. Rev. Lett. 27, 287 (1971).

[19]G. J. Salamo, H. M. Gibbs, and G. G. Churchill, Phys. Rev. Lett. 33, 273 (1974).

[20]S. L. McCall and E. L. Hahn, Phys. Rev. 183, 457 (1969).

[21]C. K. Rhodes and A. Szoke, Phys. Rev. 184, 25 (1969).

[22]C. L. Tang and H. Statz, Appl. Phys. Lett. 10, 145 (1967).